The Nature of the Metal–Silicon Bond in $[M(SiR_3)H_3(PPh_3)_3]$ (M = Ru, Os) and the Crystal Structure of $[Os\{Si(N\text{-pyrrolyl})_3\}H_3(PPh_3)_3]$

Klaus Hübler,* Ute Hübler, Warren R. Roper,* Peter Schwerdtfeger and L. James Wright

Abstract: The compounds $[M(SiR_3)H_3(PPh_3)_3]$ (**1**: M = Ru, R = 1-NC_4H_4 = pyr; **2a–c**: M = Os, R = pyr, Et, Ph) are prepared through reaction of either $[RuH_2(PPh_3)_4]$ or $[OsH_4(PPh_3)_3]$ with the appropriate silane $HSiR_3$ (**3a–c**: R = pyr, Et, Ph). The X-ray structure analysis of compound **2a** and ab initio calculations on the model compounds $[Os(SiR_3)H_3(PH_3)_3]$ (**4a–c**: R = H, NH_2, pyr) reveal a trigonal distortion along the Os–Si axis from an idealised tetrahedral geometry for the central $OsSiP_3$ heavy-atom skeleton. The structure can be described as two face-shared octahedra, one based on osmium (OsH_3P_3) and the other based on silicon (SiH_3N_3). Studies of the bonding situation in **2a** reveal that the *N*-pyrrolyl substituents have a marked shortening effect on the osmium–silicon distance (229.3(3) pm) and that each of the three hydride ligands participates in partial three-centre bonding involving osmium, silicon and hydrogen. ^1H, ^{13}C, ^{29}Si and ^{31}P NMR spectra were used to determine the solution structures of complexes **1** and **2a**.

Keywords
ab initio calculations · hydrides · osmium · ruthenium · silicon

Introduction

The study of transition-metal silyl complexes in general and the nature of the metal–silicon bonding in particular are areas of great current interest. This is driven in part by the relevance of metal–silicon intermediates in transition-metal catalysed processes of technical importance such as hydrosilylation and the dehydrogenative polymerisation of silanes.[1, 2] One of the principal routes for the formation of a metal–silicon bond involves the reaction of a silane and a low-oxidation-state metal complex. These oxidative additions of a silane to a metal fragment can be considered in the following ways: i) two separate single bonds from the metal centre to silicon and to hydrogen, as in **I**, ii) an η^2-bonded silane adduct (or a three-centred interaction), as in **II**. These bonding situations have been extensively reported and reviewed by Schubert.[3]

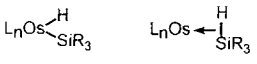

I **II**

The extent of the interaction between silicon and hydrogen within a complex is important in determining its catalytic activity. $[Ru(SiMe_3)H_3(PMe_3)_3]$, for example, has been shown to promote the dehydrogenative coupling of trimethylsilane in cyclohexane at 150 °C to give oligomeric carbosilanes with alternating silicon and carbon atoms,[4] which in turn can be utilised as precursors for the synthesis of polycarbosilanes. Very similar compounds of the composition $[M(SiR_3)H_3(PR'_3)_3]$ have been described for both ruthenium with a broad range of alkyl,[5] aryl,[5, 6] alkoxy[5, 6] or halogeno[6] substituents on silicon, and for iron with a diphenylmethylsilyl ligand.[7] The structural characterisation of the analogous triphenylstannyl iron complex $[Fe(SnPh_3)H_3(PEtPh_2)_3]$,[7] as well as of the cationic $[OsH_3(PPh_3)_4]^+$,[8] have shown that these species contain nearly tetrahedral $FeSnP_3$ and OsP_4 cores, respectively. Unfortunately, X-ray structure analyses could not reveal the positions of the hydride ligands directly bound to the metal centre for any of these compounds. To our knowledge no analogous osmium derivatives have yet been reported. Only very recently Esteruelas and coworkers published the synthesis and X-ray structure of $[Os(SiHPh_2)H_3(CO)(PiPr_3)_2]$, the first trihydridosilyl osmium complex, prepared by oxidative addition of diphenylsilane to a dihydrido–olefin complex.[9] However, the asymmetric positions of the hydride ligands could only be established by ab initio calculations.

Another feature addressed in this study is the special role played by the *N*-pyrrolyl substituents on silicon. Recent studies have demonstrated that *N*-pyrrolyl-substituted phosphines have unusual ligand properties. Tri-*N*-pyrrolyl phosphine has the attributes of a good π acceptor ligand, as revealed by spectroscopic and structural studies of compounds involving this ligand.[10]

In this paper we describe the synthesis of the compounds $[M(SiR_3)H_3(PPh_3)_3]$ (M = Ru, Os) and their characterisation

[*] Dr. K. Hübler, Dr. U. Hübler, Prof. W. R. Roper, Prof. P. Schwerdtfeger, Dr. L. J. Wright
Department of Chemistry, The University of Auckland
Private Bag 92019, Auckland (New Zealand)
Fax: (9) 3737-422
e-mail: w.roper@auckland.ac.nz

0947-6539/97/0310-1608 $ 17.50+.50/0

by standard analytical methods, as well as the solid-state structure of osmium complex **2a** and theoretical calculations on its corresponding model compounds, including analyses concerned with the bonding situation between silicon, osmium and the three hydride ligands.

Results and Discussion

The seven-coordinate compounds $[M(SiR_3)H_3(PPh_3)_3]$ (M = Ru, Os) can be prepared easily from $[RuH_2(PPh_3)_4]$[11] or $[OsH_4(PPh_3)_3]$[12] and the appropriate silane in toluene or benzene, respectively. For the reactions involving tri-*N*-pyrrolylsilane,[13] the complexes $[Ru\{Si(pyr)_3\}H_3(PPh_3)_3]$ (**1**; pyr = 1-NC_4H_4) and $[Os\{Si(pyr_3)\}H_3(PPh_3)_3]$ (**2a**) form after 30 min and 4 h, respectively, at 80 °C whereas the analogous osmium triethyl- and triphenylsilyl derivatives (**2b,c**) can be synthesised only after 3 days and one week, respectively, of heating under reflux (Scheme 1). After the appropriate reaction

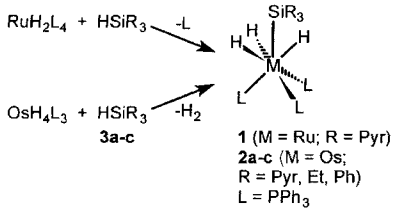

Scheme 1. Complexes **1** and **2a** form under relatively mild conditions, whereas the analogous complexes **2b** and **2c** require long periods of heating under reflux.

time the compounds precipitate from benzene/*n*-hexane as almost colourless solids, which are fairly stable to oxygen and moisture. The tri-*N*-pyrrolylsilyl complexes **1** and **2a** are surprisingly stable and do not add carbon monoxide even under 400 kPa pressure at 60 °C. Complex (**2a**) is stable both to tetrafluoroboric acid and to sodium hydroxide. In the following section, the spectroscopic properties of compounds **1** and **2a** are discussed. Very similar results are obtained for **2b** and **c**.

Abstract in German: *Die Verbindungen $[M(SiR_3)H_3(PPh_3)_3]$ (**1**: M = Ru, R = 1-NC_4H_4 = pyr; **2a–c**: M = Os, R = pyr, Et, Ph) können durch Reaktion von $[RuH_2(PPh_3)_4]$ oder $[OsH_4(PPh_3)_3]$ mit dem entsprechenden Silan $HSiR_3$ (**3a–c**: R = pyr, Et, Ph) hergestellt werden. Die Auswertung einer Röntgenstrukturanalyse von Komplex **2a** wie auch ab-initio-Berechnungen an den Modellverbindungen $[Os(SiR_3)H_3(PH_3)_3]$ (**4a–c**: R = H, NH_2, pyr) ergeben ein entlang der Os–Si-Achse gedehntes Tetraeder für die zentrale $OsSiP_3$-Einheit. Unter Berücksichtigung der Hydrid-Liganden kann die Struktur auch als zwei flächenverknüpfte Oktaeder an Osmium (OsH_3P_3) und Silizium (SiH_3N_3) aufgefaßt werden. Untersuchungen der Bindungsverhältnisse in **2a** ergeben, daß die N-Pyrrolyl Substituenten den Os–Si Bindungsabstand signifikant verkürzen und daß jeder der drei Hydrid-Liganden an einer partiellen Drei-Zentren-Bindung zwischen Osmium, Silizium und Wasserstoff teilnimmt. Die Struktur der Komplexe **1** und **2a** in Lösung wird durch Auswertung der ^1H-, ^{13}C-, ^{29}Si- und ^{31}P-NMR-Spektren ermittelt.*

IR and NMR spectra: The IR spectrum of **1** shows two bands for the antisymmetric and symmetric RuH_3 stretches at $\tilde{\nu} = 1969$ and 1960 cm^{-1}. For the osmium complex **2a** three bands are found for the corresponding OsH_3 modes at 2055, 2043 and 2029 cm^{-1}. The appearance of three bands is a result of solid-state splitting, since in dichloromethane solution only one broad band at 2054 with a shoulder at 2061 cm^{-1} is observed. In addition to these ν(MH) bands, a characteristic absorption at 1183 cm^{-1} in the spectra of **1** and **2a** is found for the tri-*N*-pyrrolylsilyl ligand bound to a metal centre.

At room temperature, the $^{31}P\{^1H\}$ NMR spectra of **1** and **2a** show only one singlet in each case (at $\delta = 32.2$ and -0.3, respectively), which are broadened in the proton-coupled ^{31}P spectra. In the ^1H NMR spectra only one resonance is observed for the three hydride ligands (at $\delta = -9.80$ and -10.64, respectively; Figure 1), along with the expected signals for the triphenylphos-

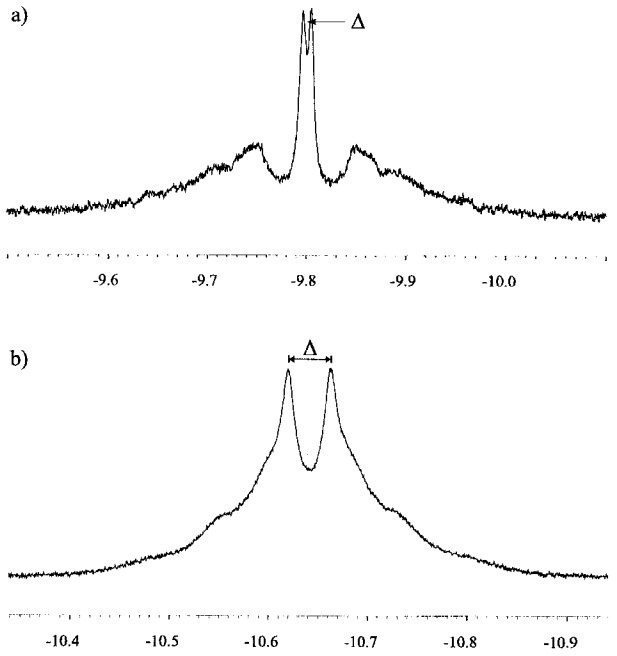

Figure 1. High-field region of the ^1H NMR spectrum measured in $[D_8]$toluene of $[Ru\{Si(pyr)_3\}H_3(PPh_3)_3]$ (**1**; spectrum a) and $[Os\{Si(pyr)_3\}H_3(PPh_3)_3]$ (**2a**; spectrum b) showing the AA'A" part of an AA'A"XX'X" spectrum with the two main lines separated by Δ.

phine groups and for one set of pyrrolyl rings. These observations suggest that, at least on the NMR timescale, the complexes have C_3 symmetry. Likely structures have either an eclipsed (trigonal prismatic, **III**) or a staggered (octahedral, **IV**) arrangement of hydride and phosphine ligands. To exclude the possibility of a nonclassical hydride complex, that is, a dihydrogen adduct, the ^1H NMR spectra were recorded between -85 and $+25$ °C. No significant changes to the relevant peaks were observed. In addition, measurements of the spin lattice relaxation times t_1 at room temperature give values of 278 and 310 ms at 400 MHz, suggesting that **1** and **2a** are classical

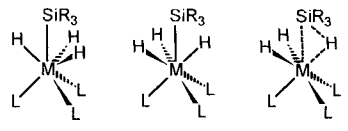

  0947-6539/97/0310-1609 $ 17.50+.50/0

trihydride complexes.[9, 14–16] The appearance of only one sharp singlet in the high-field region of the $^1H\{^{31}P\}$ NMR spectra for both **1** and **2a** confirms that the pattern of the signals depicted in Figure 1 is due only to coupling with the three phosphorus atoms.

With the help of NMR-simulating software the signals could be shown to feature the AA′A″ part of an AA′A″XX′X″ spectrum. For this type of spin system, the difference between the two main lines (Δ, Figure 1) equals the absolute value of the sum of the three coupling constants between A (protons) and the three magnetically different X (phosphorus) nuclei. Thus, Δ is either $|^2J(H,P_{cis}) + 2^2J(H,P_{trans})|$ or $|^2J(H,P_{trans}) + 2^2J(H,P_{cis})|$ for the two possible arrangements **III** and **IV**. In mixed hydride phosphine complexes the proton–phosphorus coupling constants usually correlate with the bonding angle between the participating atoms. For example in $[OsHCl(CO)(PPh_3)_3]$ or $[RuHCl(CO)(PPh_3)_3]$, absolute values of 87.6 or 106.1 Hz for $^2J(H,P_{trans})$ and 24.5 or 23.8 Hz for $^2J(H,P_{cis})$ are observed. The very small line separations Δ of 2.8 and 16.0 Hz observed in the spectra of **1** and **2a** can therefore only be produced by the sum $|^2J(H,P_{trans}) + 2^2J(H,P_{cis})|$ with one of the coupling constants having a negative sign. This fixes the geometry on the osmium centre as that shown in **IV** and eliminates **III** as a possibility. Unlike the situation observed for $[Fe(SnPh_3)H_3(PEtPh_2)_3]$[7] the hydride resonances did not change on cooling to the lowest experimentally accessible temperature of −85 °C. Thus there is no support for the formation of the η^2-silane dihydride species **V**, although this arrangement cannot be ruled out.

The $^{29}Si\{^1H\}$ NMR spectra of **1** and **2a** show the expected quartets at $\delta = 8.6$ and 8.3, respectively, with corresponding $^2J(Si,P)$ parameters of 14.6 and 14.1 Hz. The proton-coupled ^{29}Si NMR spectrum of the ruthenium derivative **1** is clearly recognizable as a quartet of quartets with a $J(Si,H)$ of 47.4 Hz. This pattern is consistent with coupling to three equivalent hydrogen atoms. The proton-coupled ^{29}Si NMR spectrum of the osmium derivative **2a** is a complex multiplet, not immediately recognizable as a quartet of quartets, but which has been simulated as such with $J(Si,H)$ of 29.2 Hz.

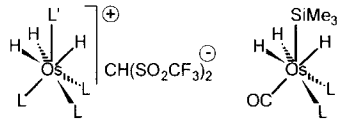

5; L = L′ = PPh_3 **9**; L = PPh_3

A very similar complex is found in the cation of $[OsH_3(PPh_3)_4][HC(SO_2CF_3)_2]$ (**5**).[8] The ^1H NMR spectrum of this compound shows a quintet for the hydride ligands at room temperature, which only collapses at −60 °C. The $^{31}P\{^1H\}$ NMR spectrum at −80 °C shows two singlets in a 3:1 ratio for two different groups of phosphorus atoms that coalesce to only one signal above −60 °C. This means that **5** undergoes a fluxional process that rapidly equilibrates the four PPh_3 ligands on the NMR timescale at temperatures above −60 °C. For the tris(triphenylphosphine)silyl complexes **1** and **2a** there is no comparable process interchanging the phosphine and silyl ligands. An interaction between silicon and the three hydrides would stabilise the isomer with the silyl ligand occupying the special position and could therefore be the reason for this observation.

Crystal structure of 2a: The crystal structure of **2a** contains one $[Os\{Si(pyr_3)\}H_3(PPh_3)_3]$ complex and three independent chloroform molecules per asymmetric unit. Figure 2 shows the coordination sphere of osmium with almost perfect C_3 symmetry about the Os–Si axis. Complete bond lengths and angles for the N_3SiOsP_3 skeleton are presented in Table 1; for comparison with the calculations discussed below, only average distances and angles are given in Table 2.

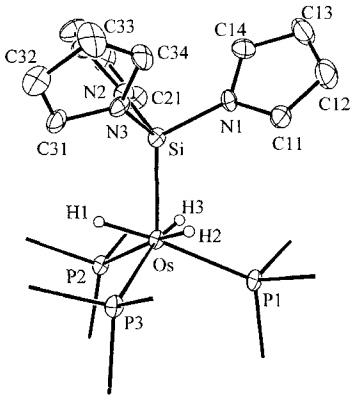

Figure 2. Molecular structure of $[Os\{Si(pyr)_3\}H_3(PPh_3)_3]$ (**2a**). For clarity, the phenyl rings of the triphenylphosphine groups and all hydrogen atoms are omitted, except the hydride ligands directly bonded to the osmium centre.

Table 1. Complete distances (pm) and angles (°) for the N_3SiOsP_3 skeleton of $[Os\{Si(pyr)_3\}H_3(PPh_3)_3]$ (**2a**).

	$x = 1$	$x = 2$	$x = 3$	av.
Nx–Si	179.2(10)	178.0(10)	177.3(10)	178.2
Nx-Si-Os	118.5(4)	117.5(4)	117.8(4)	117.9
Nx-Si-N(x+1)	99.7(5)	100.1(5)	99.7(5) [a]	99.8
Px–Os	242.7(3)	244.1(3)	244.2(3)	243.7
Px-Os-Si	112.9(1)	114.5(1)	113.9(1)	113.8
Px-Os-P(x+1)	104.3(1)	105.0(1)	105.4(1) [a]	104.9
Px-Os-Si-Nx	−7.6(4)	−6.9(4)	−7.8(4)	−7.4

[a] When $x = 3$, $x + 1 = 1$.

Table 2. Selected interatomic distances (pm) and angles (°) for $[Os\{Si(pyr)_3\}H_3(PPh_3)_3]$ (**2a**) and the model compounds $[Os(SiR_3)H_3(PH_3)_3]$ (**4a–c**: R = H, NH_2, pyr).

	2a (X = N) [a]	**4a** (X = H)	**4b** (X = N)	**4c** (X = N)
method	X-ray	MP2	MP2	MP2
Os–Si	229.3(3)	241.4	243.6	231.3
Os–P	243.7	235.4	234.8	236.7
Si–X	178.2	147.8	173.2	176.8
Os–H	–	165.0	164.7	164.6
Si···H	–	215.7	214.2	210.0
Os-Si-X	117.9	113.7	112.6	115.6
X-Si-X	99.8	104.9	106.2	102.7
Si-Os-P	113.8	118.9	118.6	118.6
P-Os-P	104.9	98.6	99.0	99.0
Si-Os-H	–	60.7	59.6	61.4
P-Os-H_{trans}	–	179.6	178.1	178.8
H-Os-H	–	98.1	96.7	99.0
X-Si-Os-P_{cis}	−7.4	−0.1	−8.0	−0.7
X-Si-Os-H_{trans}	–	−180.1	−187.3	−179.4
P-Os-Si-H_{trans}	–	−180.0	−180.7	−181.3

[a] Since the X-ray structure of compound **2a** shows it to have almost perfect C_3 symmetry (see Table 1), average distances, angles and torsion angles are shown in this table.

0947-6539/97/0310-1610 $ 17.50+.50/0 *Chem. Eur. J.* **1997**, *3*, No. 10

With an average angle of 104.9° between any two phosphine ligands and 113.8° between silicon and any one phosphine ligand, the $OsSiP_3$ unit is significantly distorted along the Os–Si vector from an idealised tetrahedral geometry. This points to the three hydride ligands each capping one of the three SiP_2 faces of the distorted tetrahedron. When including the hydride ligands on osmium in the positions indicated by the ab initio calculations (see below) as well as the nitrogen atoms on silicon, the structure can be described as two octahedral coordination polyhedra, one based on osmium (OsH_3P_3) and the other on silicon (SiH_3N_3), with a face-sharing H_3 moiety. When considered in this way, the eclipsed conformation of the pyrrolyl groups with respect to the triphenylphosphine ligands (tors(N-Si-Os-P_{cis}) = −7.4°) is easily understood.

The average Os–P distance of 243.7 pm is very similar to the one found for compound **5** of 243.0 pm[8] and significantly longer than the standard value of 239.3 pm (mean value for 17 published compounds[17]). This can be explained by a structural *trans* influence of the hydride ligands, and has been observed for compounds like $[RuHCl(CO)(PMePh_2)_3]$, in which the two chemically different methyldiphenylphosphine ligands show Ru–P bond lengths of 235.8 (*cis* to hydride; average) and 244.9 pm (*trans* to hydride).[18] More surprising than the relatively long Ru–P distance is the exceptionally short Os–Si bond length of 229.3 pm, which is the first under 230 pm ever to be reported.[19] Comparable parameters of 231.9 and 231.8 pm have been reported for the two hydroxysilyl complexes **6** and **7**,[20] respectively, as well as for the triosmium cluster **8** (232 pm).[21] Even the base-stabilised silylene complex

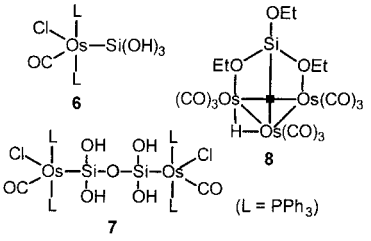

$[Os=\{SiEt_2(thf)\}(thf)(ttp)]$ (thf = tetrahydrofuran, ttp = tetra-*p*-tolylporphyrin) shows a longer Os–Si distance of 232.5 pm.[22]

Although the triphenylphosphine and the tri-*N*-pyrrolylsilyl ligands make similar steric demands, no disorder in the solid-state structure was apparent. This is compatible with the lack of fluxional behaviour deduced from the solution NMR spectra. Thus, electronic reasons might be behind this arrangement. If, however, there is any interaction between silicon and the three hydrides, this should result in a lengthening of the Si–N bonds, and, with an average value of 178.2 pm, they are indeed remarkably long compared with the 172.9 pm detected for the parent silane $HSi(pyr)_3$ (Table 3).[13] A comparison of **2a** with $[Os(SiMe_3)H_3(CO)(PPh_3)_2]$ (**9**),[23] for which larger Si-Os-P and Si-Os-C angles of 122.2° (average) and 107.9° as well as smaller values of 100.2° (average) and 100.4° for C-Os-P and P-Os-P suggest that the hydride ligands are bent towards the trimethylsilyl group here too, shows rather long Os–Si (245.3) and relatively short Os–P bonds (238.7 pm).

Table 3. Selected bond lengths (pm) and angles (°) for tri-*N*-pyrrolylsilane (**3a**) and the model compounds $HSiR_3$ (**10a**, **10b**: R = H, NH_2).

	3a (X = N)	**10a** (X = H)	**10b** (X = N)	**3a** (X = N)
method	X-ray	MP2	MP2	MP2
H–Si	136(4)	146.8	146.6	145.2
Si–X	172.9(4)	146.8	172.0	173.4
H-Si-X	110(2)	109.5	109.2	110.4
X-Si-X	109.0(2)	109.5	109.7	108.6

To clarify the role of the hydride ligands as well as the influence of the substituents on silicon for the bonding situation, ab initio calculations on various model compounds were performed.

Ab initio calculations: Geometry optimisations were carried out for each of the three model compounds $[Os(SiR_3)H_3(PH_3)_3]$ (**4a–c**: R = H, NH_2, pyr) as well as for the parent silanes $HSiR_3$ (**10a**, **10b**, **3a**: R = H, NH_2, pyr). The agreement with the experimentally obtained data is shown in Tables 2 and 3. The more technical details of the calculations can be found under Computational Details in the Experimental Section.

The calculations on the simplest model $[Os(SiH_3)H_3(PH_3)_3]$ (**4a**) followed the usual practice of replacing the bulky triphenylphosphine and tri-*N*-pyrrolylsilyl groups by PH_3 and SiH_3 respectively, although we knew that bond lengths to those ligands would be rather short. Unfortunately, the Os–Si distance, which is of great importance, was more than 10 pm too long with respect to the crystallographic value of 229.3 pm for $[Os\{Si(pyr)_3\}H_3(PPh_3)_3]$ (**2a**). Therefore SiH_3 was replaced by the more complex $Si(NH_2)_3$ substituent in order to better simulate the pyrrolyl rings. However, this increased the Os–Si distance even further (Table 2). The special properties of the tri-*N*-pyrrolylsilyl ligand, which result from the lone pairs on the nitrogen atoms being involved in the aromatic system and therefore not easily available for any bonding to silicon, could only be satisfactorily represented by this ligand itself. Likewise the importance of the phenyl rings when modelling triphenylphosphine groups by PH_3 has been recognised for calculations on $[MeAuPH_3]$, $[MeAuPMe_3]$ and $[MeAuPPh_3]$.[24] The computer-intensive calculations on $[Os\{Si(pyr)_3\}H_3(PH_3)_3]$ (**4c**, Figure 3) as well as on the appropriate silane $HSi(pyr)_3$ (**3a**) yielded results in very good agreement with the data obtained from solid-state structures (Tables 2 and 3).

An important goal of the computational part of this work was the determination of the positions of the hydrides within the complexes. Theoretical studies have proven to be powerful tools for locating hydride ligands in transition-metal complexes[25] and, because of the weakness of the X-ray crystallography in this area, it is

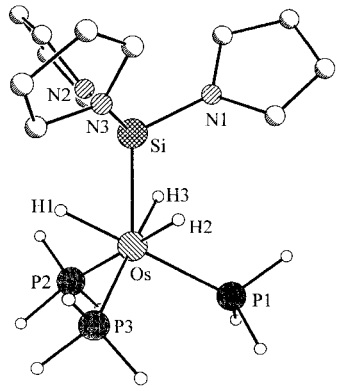

Figure 3. MP2 optimised structure of $[Os\{Si(pyr)_3\}H_3(PH_3)_3]$ (**4c**). All hydrogen atoms of the three pyrrolyl groups are omitted for clarity.

  0947-6539/97/0310-1611 $ 17.50+.50/0

not unlikely that the positions calculated for the model compounds **4a–c** are more accurate than those found in the solid-state structure of **2a**. In all calculations each hydride was found to be *trans* to one phosphine group (tors(P-Os-Si-H_{trans}) = −180.0 to −181.3°; Table 2) and *trans* to a hydrogen or to one of the pyrrolyl rings on silicon (tors(X-Si-Os-H_{trans}) = −180.1 and −179.4°) in **4a** and **4c** respectively. The largest deviation from this conformation was found for the amino derivative **4b**, which has a torsion angle N-Si-Os-H_{trans} of −187.3°.

In **4c** the Os–Si distance of 231.3 pm was only 2 pm longer than that found in the solid-state structure. Also, the angles around silicon were within 3° of the experimental values. This close correspondence of experimental and theoretical values confirms the reliability of the calculations. The lengthening of the Si–N bonds for the coordinated tri-*N*-pyrrolylsilyl group in comparison with the free silane (**4a**: 176.8 pm to **10a**: 173.4 pm) is much greater than the lengthening observed for the analogous triaminosilyl compounds (**4b**: 173.2 to **10b**: 172.0 pm). In parallel with this, the Os–Si distance for the triaminosilyl complex **4b** of 243.6 pm was found to be much longer than that in **4c** (231.3 pm). This suggests that in **4c** silicon forms stronger bonds to osmium and possibly also to the three hydride ligands, while in **4b** overlap of the lone pairs on nitrogen with silicon orbitals most likely still stabilises the Si–N bond, as this is common for aminosilanes with an available electron pair on nitrogen. The delocalisation of the nitrogen lone pairs is discussed in more detail below. From the previously discussed torsion angles N-Si-Os-H_{trans} it is clear that it is not as favourable to place the hydrides *trans* to the ancillary groups on silicon in **4b** as it is in **4a** and **4c**.

With respect to the Si–H distances, it is widely accepted that bonding interactions can be considered between silicon and hydrogen where the two atoms are separated by less than 200 pm.[3] However, the Si–H ground-state potential energy curve, with a minimum of 278 kJ mol^{-1} at 147 pm, still shows half the bond energy at a Si–H distance of ca. 220 pm.[26] This indicates that Si–H contacts of 210.0 pm in complex **4c** are still important when describing the bonding situation of silicon.

The P-Os-P angle in **4c** turns out to be slightly too small and as a result the Si-Os-P angle is overestimated by 4.8°. However, as a comparison with the parameters obtained for the SiH_3 and $Si(NH_2)_3$ models (**4a** and **4b**, respectively) clearly shows, this is not the result of an effect of the pyrrolyl rings on silicon, but rather the substitution of the PPh_3 ligands in the original compound **2a** by the far less bulky PH_3 ligands. Including the phenyl rings in our calculations would not have been feasible with current codes and computer limitations.

To study the bonding situation in more detail the natural localised molecular orbitals (NLMOs)[27] based on natural bond orbital (NBO)[28] analyses were computed for all geometry-optimised structures by the following procedure. First, the model complexes were separated into three H^- units and a central $[Os(SiR_3)(PH_3)_3]^{3+}$ core with no bonds between any of these parts and, if applicable, one lone pair at each nitrogen atom. Figure 4 shows an electron isodensity contour map for the σ*(Os–Si) orbital of the central $[Os(SiR_3)(PH_3)_3]^{3+}$ unit. This is justified because hydrogen atoms on transition metals such as osmium usually carry a partial negative charge. In a second step the system was allowed to delocalise. Figures 5 and 6 show an electron isodensity contour map and a qualitative bonding picture for the delocalisation of the hydride electrons for the example of the SiH_3 complex **4a**. Table 4 summarises the results for the analyses of **4a–c** as well as comparable values for the corresponding free silanes $HSiR_3$ (**10a**, **10b**, **3a**: R = H, NH_2, pyr).

The population analyses indicate no significant changes when comparing charges and populations of the bound silyl ligands

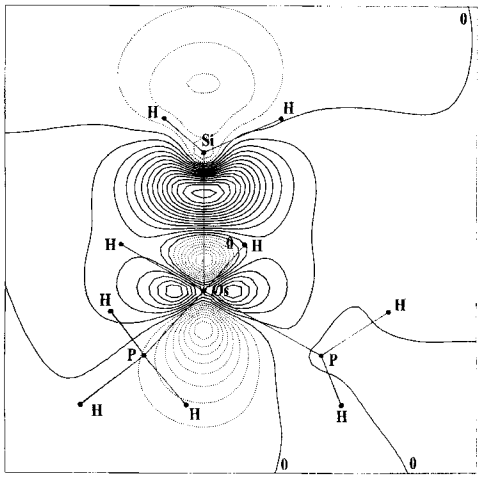

Figure 4. Contour plot of the natural bond orbital (NBO) for the σ*(Os–Si) orbital in $[Os(SiH_3)H_3(PH_3)_3]$ (**4a**) generated with the program MOLDEN.[41] Full lines designate positive and dotted lines negative values of the orbital, changing in steps of 0.02.

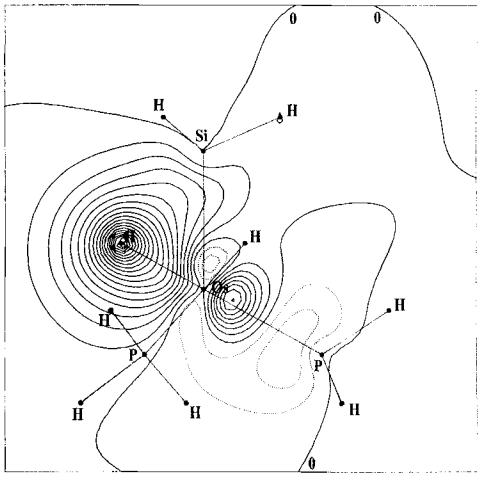

Figure 5. Contour plot of the natural localised molecular orbital (NLMO) for the delocalisation of a hydride lone pair in $[Os(SiH_3)H_3(PH_3)_3]$ (**4a**) generated with the program MOLDEN.[41] Full lines designate positive and dotted lines negative values of the orbital, changing in steps of 0.02.

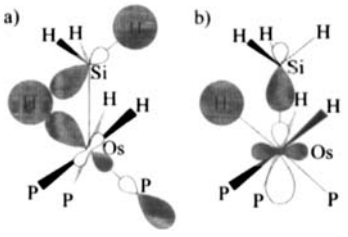

Figure 6. Qualitative picture for the delocalisation of one hydride lone pair into a) σ* orbitals of the Os–P and Si–H bonds and into b) σ* orbitals of the Os Si bond in the model complex $[Os(SiH_3)H_3(PH_3)_3]$ (**4a**).

0947-6539/97/0310-1612 $ 17.50+.50/0 Chem. Eur. J. 1997, 3, No. 10

Table 4. Results of the NBO analyses for the silanes $HSiR_3$ (**10a**, **10b**, **3a**: R = H, NH_2, pyr) as well as for the model compounds of the oxidative addition products, $[Os(SiR_3)H_3(PH_3)_3]$ (**4a–c**: R = H, NH_2, pyr).

Table 4a. Charges q, populations (popn) and second-order perturbation energies (E2 in kJ mol^{-1}) based on the NPA.[27]

	(R = H, X = H)		(R = NH_2, X = N)		(R = pyr, X = N)	
	10a	**4a**	**10b**	**4b**	**3a**	**4c**
$q_{H/Os}$	−0.23	−0.86	−0.33	−0.87	−0.27	−0.85
q_{Si}	0.91	0.93	2.16	2.19	2.22	2.18
q_X	−0.23	−0.25	−1.44	−1.45	−0.97	−0.98
q_{Hyd}	–	−0.11	–	−0.12	–	−0.09
popn($3s_{Si}$)	0.97	0.94	0.59	0.56	0.58	0.58
popn($3p_{Si}$)	2.08	2.08	1.20	1.20	1.14	1.20
popn($3d_{Si}$)	0.05	0.05	0.06	0.05	0.05	0.05
popn(lp(N))	–	–	1.94	1.94	1.68	1.66
E2[$s_{Hyd} \rightarrow \sigma^*(Os-P_{trans})$]	–	1881	–	1950	–	1880
E2[$s_{Hyd} \rightarrow \sigma^*(Os-Si)$]		632	–	499	–	875
E2[$s_{Hyd} \rightarrow \sigma^*(Si-X_{trans})$]	–	33	–	39	–	62

Table 4b. Atom–atom net linear bond orders and delocalisation of the lone pair on nitrogen as well as for the hydride electrons based on the NLMO/NPA analyses.[27]

	(R = H, X = H)		(R = NH_2, X = N)		(R = pyr, X = N)	
	10a	**4a**	**10b**	**4b**	**3a**	**4c**
BO(H/Os···Si)	0.77	0.78	0.66	0.70	0.71	0.89
BO(Si–X)	0.77	0.75	0.38	0.35	0.32	0.27
lp(N) → Si	–	–	7.2%	7.3%	4.6%	3.2%
lp(N) → 4*C	–	–	–		14.9%	16.9%
BO(Si···H)	–	0.20	–	0.19	–	0.24
BO(Os···H)	–	0.46	–	0.46	–	0.45
Hyd → Os	–	22.4%	–	22.3%	–	21.7%
Hyd → Si		9.9%	–	9.5%	–	11.8%

with those of the free silanes. It is especially noteworthy that no particular d-orbital contribution on silicon could be detected, even though silicon exceeds a coordination number of four in the complexes if weak bonding interactions are considered (Table 4a). On the other hand, there are significant differences in the bond orders (BO) and delocalisation of the lone pairs on the nitrogen atoms in the free silanes and corresponding coordinated silyl groups. While BO(Si–N) decreases only slightly from 0.38 to 0.35 and the delocalisation from the three nitrogen atoms to silicon stays approximately the same at 7.2 and 7.3% as we go from $HSi(NH_2)_3$ (**10b**) to $[Os\{Si(NH_2)_3\}H_3(PH_3)_3]$ (**4b**), the same parameters show a significantly greater decrease from 0.32 to 0.27 and from 4.6 to 3.2% for the tri-*N*-pyrrolylsilyl analogues **3a** and **3c** (Table 4b). In agreement with the observation of weakened Si–N bonds in **4c**, nitrogen is more strongly involved in the aromatic pyrrolyl system. This can be seen from the increased delocalisation towards the four carbon atoms of almost 2%. Most importantly, in **4c** silicon shows the highest bond orders to osmium (0.89) and the hydride ligands (0.24) of all three calculated complexes.

An important advantage of starting with separated parts of the molecule, namely the three hydrides each with two s electrons and the remaining osmium core, is the possibility of calculating energies for the interaction of the hydride lone pair and all other MOs on osmium and silicon through a second-order perturbation theory analysis. Besides the dominant combination with the $\sigma^*(Os-P_{trans})$ to form an Os–H σ bond in all three complexes, energetically preferable interactions are found for $\sigma^*(Os-Si)$ (Figure 4) and, less significantly, for $\sigma^*(Si-N_{trans})$ (Table 4a). Starting with the SiH_3 derivative **4a** the introduction of the highly electron-withdrawing pyrrolyl groups on silicon improves the gain in energy not only because of delocalisation of the hydride electrons (Figure 5) into $\sigma^*(Si-X)$ orbitals (33–62 kJ mol^{-1}, Figure 6a), but also owing to interaction with the $\sigma^*(Os-Si)$ orbital (632 to 875 kJ mol^{-1}, Figure 6b). The latter interaction is more important when describing the silicon hydrogen contact, and also diminishes the antibonding between osmium and silicon. It has the smallest value in **4b** (499 kJ mol^{-1}); again, this explains the rather long Os–Si distance in this compound.

The same effect can also be seen when NLMOs are formed from NBOs. Here, the hydride s orbitals (s_{Hyd}) delocalise into hybrids on osmium to almost the same extend for all three complexes **4a–c** (22.4, 22.3 and 21.7%), while the donation into silicon orbitals is considerably larger for the tri-*N*-pyrrolylsilyl derivative **4c** (11.8%) than it is for the two other model compounds (9.9 and 9.5%; Table 4b; Figure 6). This leads to a strengthening not only of the Si–H but also of the Os–Si bond, by increasing the electron density between the latter two atoms, as can nicely be seen in Figure 5. A further analysis shows that 80% of the above-mentioned bond order of 0.89 between osmium and silicon in **4c** is a result of this delocalisation process.

For the following applications (vibrational analysis, the determination of rotational barriers and energy calculations on slightly different isomers) calculations on **4c** were not feasible. In these cases the much simpler model **4a** was used.

The harmonic vibrational analysis (two slightly negative modes for PH_3 torsions which we can safely neglect) reveal bands at 2059 and 2044 cm^{-1} for the symmetric and two degenerate antisymmetric OsH_3 vibrations; this is consistent with the previously discussed experimental IR data.

The barriers calculated for the rotation of the SiH_3, OsH_3 and OsP_3 groups with respect to the Os–Si axis are 22, 199 and 179 kJ mol^{-1}. Bearing in mind that the rotational barrier for ethane is only 13 kJ mol^{-1},[29] the energy calculated for the silyl group is significantly higher than for a simple rotation around a single bond. The behaviour of the Os–Si distance and the Os–H···Si contact throughout the rotation is illustrated in Figure 7. Rotation of the SiH_3, which destroys the optimal *trans* arrangement of hydrides and hydrogen atoms on silicon, leads to a remarkable increase of 3.1 and 9.2 pm for Os–Si and Si···H, respectively. Rotation of the three phosphine groups breaks the octahedral symmetry of the OsH_3P_3 centre, and this results in an enormous lengthening of Os–Si by 10.3 pm and an even greater shortening of Si···H by 17.9 pm. The rotation of the hydrides combines both effects, and the rotational barrier of 199 kJ mol^{-1} shows convincingly that the hydride positions found with all analytical methods represent a substantial energy minimum relative to any other possible arrangement. The sensitivity of the Si···H distance to the different rotations again supports substantial interactions between silicon and the three hydrides on osmium.

Comparison of the spectroscopic properties of $[Os\{Si(pyr)_3\}H_3(PPh_3)_3]$ (**2a**) with those of the very similar compound $[OsH_3(PPh_3)_4][HC(SO_2CF_3)_2]$ (**5**)[8] shows that the latter cationic complex is fluxional in solution at room temperature, whereas **2a** is not. To estimate the extent that interactions between silicon and the three hydrides are the reason for this difference, the structure of $[Os(SiH_3)H_3(PH_3)_3]$ (**4a**) was opti-

  0947-6539/97/0310-1613 $ 17.50+.50/0

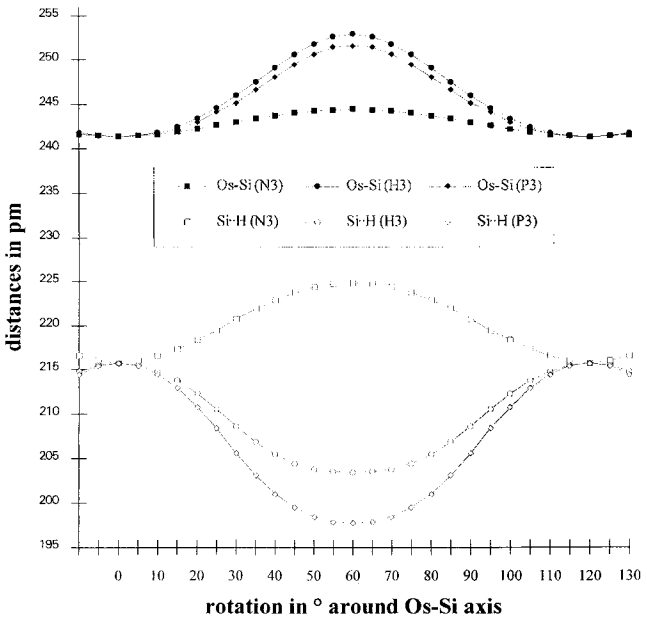

Figure 7. Study of Os–Si bond and Si···H contact distances (pm) for the rotation of the SiH_3 (N3), the OsH_3 (H3) or the OsP_3 group (P3) around the Os–Si axis in the model compound $[Os(SiH_3)H_3(PH_3)_3]$ (**4a**). An MP2 optimisation was performed at intervals of 5° from 0 to 60°.

mised again after exchanging the position of silicon with one of the phosphorus atoms and restricting the geometry as little as possible, but as much as was needed to retain P···H instead of Si···H contacts. Without any restrictions, no other local energy minima could be found besides the fully optimised structure. Figure 8 shows the optimised structures in an energy diagram.

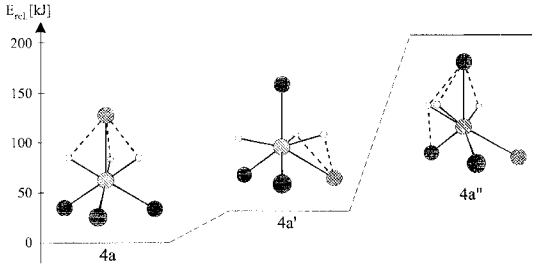

Figure 8. Energy diagram for geometry optimisations on $[Os(SiH_3)H_3(PH_3)_3]$ (**4a**) under different restrictions concerning bond angles. All atoms are marked the same way as in Figure 3. Si···H and P···H contacts smaller than 230 pm are dashed.

In a first step (**4a′**), only the bond angle between the unique phosphorus and the other silicon or phosphorus atoms was fixed at 118.9°, the value of the fully optimised complex **4a**. The total electronic energy then rose by 32 kJ mol^{-1} with two hydrides still bent towards the silicon. Thus, in a second step (**4a′**), in addition to the previous restraints, the angle of the hydrides to the unique phosphorus was set to 60.7°. The energy increased by 207 kJ mol^{-1} with respect to the fully optimised structure **4a**. This is similar to a calculated value of 267 kJ mol^{-1} for a Si–H single bond and shows clearly that Si···H contacts are much more favourable than P···H contacts.[26]

Conclusions

NMR spectroscopy, X-ray crystallography and ab initio calculations have independently proven that $[Os\{Si(pyr)_3\}H_3(PPh_3)_3]$ is a trihydrido complex with an extraordinarily short Os–Si bond. The hydride ligands are in bridging positions and three partial Si–H–Os three-centre bonds are formed. This bonding arrangement is particularly favoured because of the special electronic nature of the pyrrolyl substituents on silicon. It arises because, although the silicon has three electronegative nitrogen atoms bound to it (strong −I), the free electron pairs on the nitrogen atoms are mostly delocalised in the aromatic systems of the five-membered rings and hence are largely unavailable for any backbonding towards silicon (weak +M). Ab initio calculations confirmed the highly electron-withdrawing nature of the pyrrolyl groups, whereas for the amino substituent on silicon the two opposing effects (− I and +M) seem to be of comparable importance. We have shown that the tri-*N*-pyrrolylsilyl group cannot be sucessfully modelled by SiH_3 or $Si(NH_2)_3$ groups for ab initio calculations. This is especially true for transition-metal complexes of this group. Analysis of the solution NMR data suggests that complexes **1** and **2** possess a very similar arrangement of substituents around the metal centres in solution compared with the solid state.

Experimental Section

General methods: All reactions were carried out by standard Schlenk techniques in a dry atmosphere of oxygen-free dinitrogen. The solvents were carefully dried and distilled from the appropriate drying agents prior to use.[30] NMR spectra were measured on a Bruker DRX400 spectrometer at 400.128 MHz (^{1}H), 100.625 MHz (^{13}C), 79.495 MHz (^{29}Si) or 161.976 MHz (^{31}P) at 25 °C, except where otherwise noted. All chemical shifts were recorded downfield from tetramethylsilane or phosphoric acid (^{31}P) on the δ scale. Infrared spectra were recorded on a Perkin-Elmer FT-IR spectrometer Paragon 1000PC. High resolution mass spectra (fast atom bombardment, FAB^+ at 8 kV) were determined on a VG 70-SE mass spectrometer. Melting points are reported in degrees Celsius (uncorrected). Analytical data were obtained from the Microanalytical Laboratory, University of Otago. Evidence of solvation of some analytical samples was apparent from the ^{1}H NMR spectrum (H_2O: $\delta = 1.58$ (s), CH_2Cl_2: 5.29 (s)). Compounds $[RuH_2(PPh_3)_4]$,[11] $[OsH_4(PPh_3)_3]$[12] and tri-*N*-pyrrolylsilane[13] were all prepared according to literature procedures.

X-ray structure analyses of 2a·3CHCl$_3$: $C_{69}H_{63}Cl_9N_3OsP_3Si$, $M = 1564.47$ g mol^{-1}; data collection: Siemens Smart CCD, $\lambda(Mo_{K\alpha}) = 71.069$ pm; crystal dimensions $0.15 \times 0.2 \times 0.2$ mm^3, colourless blocks, SADABS absorption correction, $T = 203(2)$ K; triclinic, space group $P\bar{1}$ (No. 2[31a]), $a = 1239.7(6)$, $b = 1319.7(9)$, $c = 2194(2)$ pm, $\alpha = 103.15(4)$, $\beta = 101.97(3)$, $\gamma = 95.77(4)$°, $V = 3379(4) \times 10^6$ pm^3, $\rho_{calcd} = 1.538$ g cm^{-3}, $Z = 2$, $\mu(Mo_{K\alpha}) = 2.376$ mm^{-1}, scan range: $1.0 \le \theta \le 25$°; 11775 independent reflections, 10884 observed reflections, 7664 independent reflections with $F_o > 4\sigma(F_o)$; 744 parameters; 18 restraints; $R_1 = 7.9$, $wR_2 = 0.184$, GooF = 1.07, electron density: min = −2.82, max = 5.92×10^{30} e$^-$ m^{-3}; the structure was solved by Patterson methods and the refinement on F^2 was carried out by full-matrix least-squares techniques with the SHELXTL program system.[31b] All non-hydrogen atoms were anisotropically refined except C115, C116 and the atoms of the chloroform solvent molecules. All hydrogen atoms were calculated in optimised positions with $U_{iso} = 1.2\,U_{eq}(C)$. Crystallographic data (excluding structure factors) for the structure reported in this paper have been deposited with the Cambridge Crystallographic Data Centre as supplementary publication no. CCDC-100049. Copies of the data can be obtained free of charge on application to The Director, CCDC, 12 Union Road, Cambridge CB2 1EZ, UK (Fax: Int. code +(1223)336-033; e-mail: deposit@chemcrys.cam.ac.uk).

0947-6539/97/0310-1614 $ 17.50+.50/0

Computational methods: All calculations were performed with the GAUSSIAN 94[32] program series including its built-in NBO[28] routines. The structures were fully optimised by means of ab initio methods with introduction of correlation energy through second-order Møller–Plesset (MP2) perturbation theory,[33] as well as gradient-corrected density functionals applying Beckes' 1988 exchange functional[34] and the correlation functional of Lee, Yang and Parr.[35] After a number of tests with different basis sets, it was decided to use the MP2 approach based on single-reference Hartree–Fock. This achieved much better results compared with experimental data than the DFT-based BLYP methodology. At first, the optimisations were carried out without any symmetry restrictions starting from different geometries, including the coordinates obtained from the X-ray analysis. Since the resulting optimised complexes showed almost perfect C_3 symmetry, subsequent calculations were performed with the corresponding symmetry restrictions. Effective core potentials were used to represent the 60 innermost electrons of the osmium atom,[36] as well as the 10-electron core of the silicon and phosphorus atoms.[37] The valence double-ζ basis sets with a (341/321/21) or a (21/21) contraction, for osmium or silicon and phosphorus respectively, were those associated to the pseudopotentials (LANL2DZ basis set[32]), supplemented with a polarisation d shell for the two third-period elements.[38] Carbon and nitrogen atoms were described with the Dunning/Huzinaga full double-ζ basis sets, which used a (721/41) contraction.[39] For the hydrogen atoms a set of 31 contracted basis functions[40] was used with an additional polarising p-function[40] for the hydrides directly attached to the osmium centre. For compound **4c** this resulted in 589 primitive gaussians contracted to 266 functions that used 240 Mbyte of memory and 11.3 Gbyte of diskspace on a multiprocessor SIC R 10000. The CPU time for one geometry cycle was 24 h on four processors. Rotational barriers were calculated on the model compound $[Os(SiH_3)H_3(PH_3)_3]$ at the MP2 level by rotation of one of the groups SiH_3, OsH_3 or OsP_3 in 5° intervals and fixing of the torsion angle between the two others to their optimised value of either 0 or 180° with respect to the Os–Si axis.

$[Ru\{Si(pyr)_3\}H_3(PPh_3)_3]$ (1): $HSi(pyr)_3$ (200 μL, 0.332 g, 1.46 mmol) was added to a suspension of $[RuH_2(PPh_3)_4]$ (0.214 g, 0.186 mmol) in dry toluene (15 mL), and the mixture was heated under reflux for 0.5 h. The solution was then concentrated under vacuum and, after addition of 15 mL *n*-hexane, a white solid was formed. Recrystallisation from CH_2Cl_2/*n*-hexane gave pure **1** (0.190 g, 0.170 mmol, 92%). Decomp 192 °C; ^{1}H NMR ($CDCl_3$): $\delta = 7.25$–6.7 (m, 45H; $P(C_6H_5)_3$), 5.81 (br, 6H; α-H, pyr), 5.79 (br, 6H; β-H, pyr), −10.20 (d', $^2J(H,P_{trans}) + 2\,^2J(H,P_{cis}) = 2.7$ Hz, 3H; RuH); slightly different values in [D$_8$]toluene: $\delta = -9.80$ (d', $^2J(H,P_{trans}) + 2\,^2J(H,P_{cis}) = 2.8$ Hz, 3H; RuH); ^{13}C{^{1}H} NMR ($CDCl_3$): $\delta = 141.2$ (br; *i*-C_6H_5), 133.8 (s; *m*-C_6H_5), 129.0 (s; *p*-C_6H_5), 127.8 (s; *o*-C_6H_5), 124.1 (br; β-*C*, pyr), 109.7 (br; α-*C*, pyr); ^{29}Si{^{1}H} NMR ($CDCl_3$): $\delta = 8.6$ (q, $^2J(Si,P) = 14.6$ Hz); ^{29}Si NMR ($CDCl_3$): $\delta = 8.6$ (qq, $^2J(Si,P) = 14.6$ Hz, $J(Si,H) = 47.4$ Hz); ^{31}P NMR ($C_6D_5CD_3$): $\delta = 32.2$ (s); IR (Nujol): $\tilde{\nu} = 1969$ (Ru–H), 1960 (Ru–H), 1183 cm^{-1} (Si–pyr$_3$); MS: *m/e* (%): 888 (44) $[Ru\{P(Ph)_3\}_3H^+]$, 263 (100) $[P(Ph_3)_3H^+]$; $C_{66}H_{60}N_3SiP_3Ru \cdot 5.5CH_2Cl_2$ (1578.42): calcd C 54.38, H 4.17, N 2.74; found C 54.46, H 4.14, N 2.86.

$[Os\{Si(pyr)_3\}H_3(PPh_3)_3]$ (2a): $HSi(pyr)_3$ (50 μL, 0.083 g, 0.365 mmol) was added to a suspension of $[OsH_4(PPh_3)_3]$ (0.104 g, 0.106 mmol) in dry benzene (10 mL). After 4 h at 80 °C the suspension had turned to a red-brown solution. The reaction was allowed to cool to room temperature. After reducing the solvent to approximately 3 mL and the addition of *n*-hexane (15 mL) a grey solid was obtained, which was collected and recrystallised from CH_2Cl_2/*n*-hexane to give pure **2a** (0.105 g, 0.087 mmol, 82%). Decomp 198 °C; ^{1}H NMR ($CDCl_3$): $\delta = 7.35$–6.6 (m, 45H; $P(C_6H_5)_3$), 5.8 (br, 12H; α- + β-H, pyr), −11.0 (d', $^2J(H,P_{trans}) + 2\,^2J(H,P_{cis}) = 17.5$ Hz, 3H; OsH); slightly different values in [D$_8$]toluene: $\delta = -10.68$ (d', $^2J(H,P_{trans}) + 2\,^2J(H,P_{cis}) = 16.0$ Hz, 3H; OsH); ^{13}C NMR ($CDCl_3$): $\delta = 140.9$ (br; *i*-C_6H_5), 133.7 (s; *m*-C_6H_5), 129.1 (s; *p*-C_6H_5), 127.7 (s; *o*-C_6H_5), 123.9 (br; β-*C*, pyr), 109.6 (br; α-*C*, pyr); ^{29}Si{^{1}H} NMR ($CDCl_3$): $\delta = 8.3$ (q, $^2J(Si,P) = 14.1$ Hz); ^{29}Si NMR ($CDCl_3$): $\delta = 8.6$ (qq, $^2J(Si,P) = 14.6$ Hz, $J(Si,H) = 29.2$ Hz); ^{31}P NMR ($C_6D_5CD_3$): $\delta = -0.3$ (s); IR (Nujol): $\tilde{\nu} = 2055$ (Os–H), 2043 (Os–H), 2029 (Os–H), 1183 cm^{-1} (Si–pyr$_3$); MS: *m/e* (%): 1208 (8) $[MH^+]$, 976 (100) $[Os(PPh_3)_3H^+]$; $C_{66}H_{60}N_3SiP_3Os \cdot 1.5H_2O$ (1233.46): calcd C 64.27, H 5.15, N 3.41; found C 64.17, H 5.45, N 3.47.

$[Os(SiEt_3)H_3(PPh_3)_3]$ (2b): A Schlenk tube containing $[OsH_4(PPh_3)_3]$ (0.118 g, 0.120 mmol) and $HSiEt_3$ (200 μL, 0.146 g, 1.26 mmol) in dry benzene (15 mL) was evacuated and sealed; the mixture was stirred for three days at 80 °C. The clear solution was then evaporated to dryness and the product recrystallised from CH_2Cl_2/*n*-hexane to yield pure **2b** (0.124 g, 0.113 mmol, 94%). M.p. 162 °C; ^{1}H NMR ($CDCl_3$): $\delta = 7.6$–6.9 (m, 45H; $P(C_6H_5)_3$), 1.04 (t, $^3J(H,H) = 7.4$ Hz, 9H; $Si(CH_2CH_3)_3$), 0.65 (q, $^3J(H,H) = 7.4$ Hz, 6H; $Si(CH_2CH_3)_3$), −11.35 (d', $^2J(H,P_{trans}) + 2\,^2J(H,P_{cis}) = 13.9$ Hz, 3H; OsH); ^{13}C NMR ($CDCl_3$): $\delta = 141.0$ (br; *i*-C_6H_5), 133.9 (s; *m*-C_6H_5), 128.2 (s; *p*-C_6H_5), 127.0 (s; *o*-C_6H_5), 15.9 (s; $Si(CH_2CH_3)_3$), 8.8 (s; $Si(CH_2CH_3)_3$); ^{29}Si{^{1}H} NMR ($CDCl_3$): $\delta = 17.9$ (s); ^{29}Si NMR ($CDCl_3$): $\delta = 17.9$ (br); IR (Nujol): $\tilde{\nu} = 2076$ (Os–H), 2062 (Os–H), 2052 cm^{-1} (Os–H); MS: *m/e* (%): 976 (60) $[Os\{P(Ph)_3\}_3H^+]$, 263 (100) $[P(Ph_3)H^+]$; $C_{60}H_{63}SiP_3Os \cdot 0.75CH_2Cl_2$ (1159.06): calcd C 62.95, H 5.61; found C 63.06, H 5.70.

$[Os(SiPh_3)H_3(PPh_3)_3]$ (2c): A mixture of $[OsH_4(PPh_3)_3]$ (0.132 g, 0.135 mmol) and $HSiPh_3$ (0.037 g, 0.142 mmol) in dry benzene (20 mL) was evacuated and heated at 80 °C in a sealed Schlenk tube for one week. After three days, additional $HSiPh_3$ (0.054 g, 0.207 mmol) was added. The brown suspension was filtered and the filtrate concentrated under vacuum to give crude **2c**. This was recrystallised from CH_2Cl_2/*n*-hexane to give pure **2c** (0.151 g, 0.122 mmol, 90%). M.p. 185 °C; ^{1}H NMR ($CDCl_3$): $\delta = 7.3$–6.7 (m, 60H; $P(C_6H_5)_3$ + $Si(C_6H_5)_3$), −10.6 (d', $^2J(H,P_{trans}) + 2\,^2J(H,P_{cis}) = 17.9$ Hz, 3H; OsH); ^{13}C NMR ($CDCl_3$): $\delta = 147.1$ (s; *i*-$Si(C_6H_5)_3$), 140.7 (br; *i*-$P(C_6H_5)_3$), 136.1 (s; *m*-$Si(C_6H_5)_3$), 133.8 (s; *m*-$P(C_6H_5)_3$), 128.4 (s; *p*-$P(C_6H_5)_3$), 127.2 (s; *o*-$P(C_6H_5)_3$), 126.4 (s; *o*-$Si(C_6H_5)_3$), 126.4 (s; *p*-$Si(C_6H_5)_3$); IR (Nujol): $\tilde{\nu} = 2055$ (Os–H), 2039 cm^{-1} (Os–H); MS: *m/e* (%): 976 (100) $[Os\{P(Ph)_3\}_3H^+]$, (67) $[P(Ph_3)H^+]$; $C_{72}H_{63}SiP_3Os \cdot 5CH_2Cl_2$ (1664.66): calcd C 55.57, H 4.42; found C 55.41, H 4.53.

Acknowledgements: We thank the Alexander von Humboldt-Stiftung for the award of a Feodor Lynen scholarship to K. H., and Dr. C. E. F. Rickard for collecting the data set for the crystal structure determination. Support from the AURC (Auckland) is gratefully acknowledged.

Received: January 7, 1997 [F 569]

[1] a) J. F. Harrod, *ACS Symp. Ser.* **1988**, *360*, 89; b) T. D. Tilley, *Acc. Chem. Res.* **1993**, *26*, 22.
[2] For a review see: I. Ojima in *The Chemistry of Organic Silicon Compounds* (Eds.: S. Patai, Z. Rappoport), Wiley, New York, **1989**, ch. 25.
[3] U. Schubert, *Adv. Organomet. Chem.* **1990**, *30*, 151.
[4] L. J. Procopio, D. H. Berry, *J. Am. Chem. Soc.* **1991**, *113*, 4039.
[5] H. Kono, N. Wakao, K. Ito, Y. Nagai, *J. Organomet. Chem.* **1977**, *132*, 53.
[6] R. N. Haszeldine, L. S. Malkin, R. V. Parish, *J. Organomet. Chem.* **1979**, *182*, 323.
[7] U. Schubert, S. Gilbert, S. Mock, *Chem. Ber.* **1992**, *125*, 835.
[8] A. R. Siedle, R. A. Newmark, L. H. Pignolet, *Inorg. Chem.* **1986**, *25*, 3412.
[9] M. L. Buil, P. Espinet, M. A. Esteruelas, F. J. Lahoz, A. Lledós, J. M. Martínez-Ilarduya, F. Maseras, J. Modrego, E. Oñate, L. A. Oro, E. Sola, C. Valero, *Inorg. Chem.* **1996**, *35*, 1250.
[10] K. G. Moloy, J. L. Petersen, *J. Am. Chem. Soc.* **1995**, *117*, 7696.
[11] R. O. Harris, N. K. Hota, L. Sadavoy, J. M. C. Yuen, *J. Organomet. Chem.* **1973**, *54*, 259.
[12] J. J. Levison, S. D. Robinson, *J. Chem. Soc. A* **1970**, 2947.
[13] J. L. Atwood, A. H. Cowley, W. E. Hunter, S. F. Sena, *Gov. Rep. Announce Index (U. S.)*, **1982**, *82*, 4027 [*Chem. Abstr.* **1982**, *98*, 45906q]; H. Schmidbaur, H. Schuh, *Z. Naturforsch.* **1990**, *B45*, 1679; K. Hübler, W. R. Roper, L. J. Wright, *17th International Conference on Organometallic Chemistry*, Brisbane (Australia), July 7–12 **1996**, *Program & Abstract Book*, p. 172.
[14] C. Hampton, W. R. Cullen, B. R. James, J.-P. Charland, *J. Am. Chem. Soc.* **1988**, *110*, 6918.
[15] F. Maseras, A. Lledós, M. Costas, J. M. Poblet, *Organometallics* **1996**, *15*, 2947.
[16] P. J. Desrosiers, L. Cai, Z. Lin, R. Richards, J. Halpern, *J. Am. Chem. Soc.* **1991**, *113*, 4173.
[17] F. H. Allen, O. Kennard, *3D Search and Research Using the Cambridge Structural Database*, in *Chem. Des. Autom. News*, **1993**, *8*, 1 & 31.
[18] M. Motevalli, M. B. Hursthouse, A. R. Barron, G. Wilkinson, *Acta Crystallogr.* **1987**, *C43*, 214.
[19] Even shorter distances have been observed for Os–SiF_3 and Os–$SiCl_3$ complexes. These results will be published subsequently.
[20] C. E. F. Rickard, W. R. Roper, D. M. Salter, L. J. Wright, *J. Am. Chem. Soc.* **1992**, *114*, 9682.
[21] R. D. Adams, J. E. Cortopassi, M. P. Pompeo, *Inorg. Chem.* **1991**, *30*, 2960 and **1992**, *31*, 2563.
[22] L. K. Woo, D. A. Smith, V. G. Young, Jr., *Organometallics* **1991**, *10*, 3977.

  0947-6539/97/0310-1615 $ 17.50+.50/0

[23] D. M. Salter, *The Synthesis and Reactivity of New Ruthenium and Osmium Silyl Complexes*, PhD thesis, Auckland (NZ) **1993**.
[24] O. D. Häberlen, N. Rösch, *J. Phys. Chem.* **1993**, *97*, 4970.
[25] Z. Lin, M. B. Hall, *Coord. Chem. Rev.* **1994**, *135*, 845.
[26] A. Mavridis, J. F. Harrison, *J. Phys. Chem.* **1982**, *86*, 1979.
[27] A. E. Reed, F. Weinhold, *J. Chem. Phys.* **1985**, *83*, 1736; A. E. Reed, P. v. R. Schleyer, *J. Am. Chem. Soc.* **1990**, *112*, 1434.
[28] E. D. Glendening, A. E. Reed, J. E. Carpenter, F. Weinhold, NBO Version 3.1.
[29] A. Streitwieser, Jr., C. H. Heathcock, *Introduction to Organic Chemistry*, 2nd ed., Macmillan, New York, **1981**, p. 71.
[30] D. D. Perrin, W. L. F. Armarego, *Purification of Laboratory Chemicals*, 3rd ed., Pergamon, New York, **1988**.
[31] a) *International Tables for Crystallography, Vol. A, Space-Group Symmetry* (Ed.: T. Hahn), 2nd ed., Reidel, Dordrecht (NL), **1984**; b) G. M. Sheldrick, *SHELXTL/PC*, Version 5.0, Siemens, Madison, Wisconsin, **1995**.
[32] M. J. Frisch, G. W. Trucks, H. B. Schlegel, P. M. W. Gill, B. G. Johnson, M. A. Robb, J. R. Cheeseman, T. Keith, G. A. Petersson, J. A. Montgomery, K. Raghavachari, M. A. Al-Laham, V. G. Zakrzewski, J. V. Ortiz, J. B. Foresman, J. Cioslowski, B. B. Stefanov, A. Nanayakkara, M. Challacombe, C. Y. Peng, P. Y. Ayala, W. Chen, M. W. Wong, J. L. Andres, E. S. Replogle, R. Gomperts, R. L. Martin, D. J. Fox, J. S. Binkley, D. J. Defrees, J. Baker, J. P. Stewart, M. Head-Gordon, C. Gonzalez, J. A. Pople, *Gaussian 94*, Revision D.3, Gaussian, Pittsburgh PA, **1995**.
[33] C. Møller, M. S. Plesset, *Phys. Rev.* **1934**, *46*, 618.
[34] A. D. Becke, *Phys. Rev.* **1988**, *A38*, 3098.
[35] C. Lee, W. Yang, R. G. Parr, *Phys. Rev.* **1988**, *B37*, 785; B. Miehlich, A. Savin, H. Stoll, H. Preuss, *Chem. Phys. Lett.* **1989**, *157*, 200.
[36] P. J. Hay, W. R. Wadt, *J. Chem. Phys.* **1985**, *82*, 299.
[37] W. R. Wadt, P. J. Hay, *J. Chem. Phys.* **1985**, *82*, 284.
[38] M. M. Francl, W. J. Pietro, W. J. Hehre, J. S. Binkley, M. S. Gordon, D. J. DeFrees, J. A. Pople, *J. Chem. Phys.* **1982**, *77*, 3654.
[39] T. H. Dunning, Jr., P. J. Hay, in *Modern Theoretical Chemistry* (Ed.: H. F. Schaefer, III), Plenum, New York, **1976**, p. 1 ff.
[40] R. Ditchfield, W. J. Hehre, J. A. Pople, *J. Chem. Phys.* **1971**, *54*, 724; W. J. Hehre, R. Ditchfield, J. A. Pople, *ibid.* **1972**, *56*, 2257; P. C. Hariharan, J. A. Pople, *Mol. Phys.* **1974**, *27*, 209; M. S. Gordon, *Chem. Phys. Lett.* **1980**, *76*, 163; P. C. Hariharan, J. A. Pople, *Theor. Chim. Acta.* **1973**, *28*, 213.
[41] G. Schaftenaar, Program MOLDEN 3.0, CAOS/CAMM Center (The Netherlands).

0947-6539/97/0310-1616 $ 17.50+.50/0